THE CELL METHOD FOR LINEAR ELASTICITY

by
Stephen V. Harren
http://www.harren.us

0. Contents

1. Governing Equations

In two dimensions, Hooke's Law is

$$\sigma_{ij} = L_{ijkl}\varepsilon_{kl} \ , \tag{1.1}$$

where σ_{ij} are the stress components, $\varepsilon_{ij} = (1/2)\big(u_{i,j} + u_{j,i}\big)$ are the strain components, u_i is the displacement vector, and where the comma denotes differentiation with respect to the (rectangular) coordinates. The tensor L_{ijkl} is given by

$$L_{ijkl} = \frac{E}{1+\nu}\left(I_{ijkl} + \frac{\nu^*}{1-2\nu^*}\delta_{ij}\delta_{kl}\right) \ , \qquad I_{ijkl} = \frac{1}{2}\big(\delta_{ik}\delta_{jl} + \delta_{jk}\delta_{il}\big) \ , \tag{1.2}$$

where E is Young's modulus, ν is Poisson's ratio, and δ_{ij} are the components of the two-dimensional identity matrix (*i.e.,* the Kronecker delta). Also, for plane strain,

$$\nu^* = \nu \ , \qquad \varepsilon_{zz} = 0 \ , \qquad \sigma_{zz} = \nu\big(\sigma_{xx} + \sigma_{yy}\big) \ , \tag{1.3}$$

and for plane stress,

$$\nu^* = \frac{\nu}{1+\nu} \ , \qquad \sigma_{zz} = 0 \ , \qquad \varepsilon_{zz} = -\frac{\nu}{1-\nu}\big(\varepsilon_{xx} + \varepsilon_{yy}\big) \ . \tag{1.4}$$

Written out, eqns. (1.1) and (1.2) are

$$\begin{aligned}
\sigma_{xx} &= \frac{E}{(1+\nu)(1-2\nu^*)}\big[\,(1-\nu^*)\varepsilon_{xx} + \nu^*\varepsilon_{yy}\,\big] \ , \\
\sigma_{yy} &= \frac{E}{(1+\nu)(1-2\nu^*)}\big[\,(1-\nu^*)\varepsilon_{yy} + \nu^*\varepsilon_{xx}\,\big] \ , \\
\sigma_{xy} &= \frac{E}{(1+\nu)}\ \varepsilon_{xy} \ ,
\end{aligned} \tag{1.5}$$

or inversely,

$$\begin{aligned}
\varepsilon_{xx} &= \frac{(1+\nu)}{E}\big[\,(1-\nu^*)\sigma_{xx} - \nu^*\sigma_{yy}\,\big] \ , \\
\varepsilon_{yy} &= \frac{(1+\nu)}{E}\big[\,(1-\nu^*)\sigma_{yy} - \nu^*\sigma_{xx}\,\big] \ , \\
\varepsilon_{xy} &= \frac{(1+\nu)}{E}\ \sigma_{xy} \ .
\end{aligned} \tag{1.6}$$

Now, the equilibrium equations are

$$\sigma_{ij,i} = 0 \ \text{ or } \ L_{ijkl}u_{k,li} = 0 \ , \tag{1.7}$$

where the second form follows from the symmetries of L_{ijkl}. Finally, admissible boundary conditions are to prescribe two of the four quantities u_i and $T_j = n_i\sigma_{ij}$ at each point on the boundary of the domain, where T_j is the traction vector and n_i is the outward-pointing unit normal vector on the boundary.

In polar coordinates, the strain-displacement relations are

$$\varepsilon_{rr} = u_{r,r} \ , \qquad \varepsilon_{\theta\theta} = \frac{1}{r}u_{\theta,\theta} + \frac{1}{r}u_r \ , \qquad \varepsilon_{r\theta} = \frac{1}{2}\left(\frac{1}{r}u_{r,\theta} + u_{\theta,r} - \frac{1}{r}u_\theta\right) \ , \tag{1.8}$$

and the equilibrium equations are

$$\sigma_{rr,r}+\frac{1}{r}\sigma_{r\theta,\theta}+\frac{1}{r}(\sigma_{rr}-\sigma_{\theta\theta})=0\ ,\qquad \sigma_{r\theta,r}+\frac{1}{r}\sigma_{\theta\theta,\theta}+\frac{2}{r}\sigma_{r\theta}=0\ . \tag{1.9}$$

Also, in polar coordinates, Hooke's Law is given by eqns. (1.1) through (1.6) above with r replacing x and θ replacing y.

2. Example in Rectangular Coordinates

Consider the stress field

$$\sigma_{xx}=\frac{12V}{H^3}\,(L-x)y\,,\qquad \sigma_{yy}=0\,,\qquad \sigma_{xy}=\frac{3V}{2H^3}\,(4y^2-H^2)\,, \tag{2.1}$$

which spans the rectangular domain (a cantilever beam) of Fig. 1 below. Note that

$$\int_{-H/2}^{H/2}\sigma_{xy}(L,y)\mathrm{d}y=-V\,,\qquad \int_{-H/2}^{H/2}y\sigma_{xx}(0,y)\mathrm{d}y=VL\,, \tag{2.2}$$

so that $V>0$ is the net shear force applied to the ends of the beam, and a moment VL is applied to the left end of the beam. Also, eqns. (2.1) satisfy the equilibrium eqns. (1.7) identically. With eqns. (2.1) and Hooke's Law (1.6), the strain components are

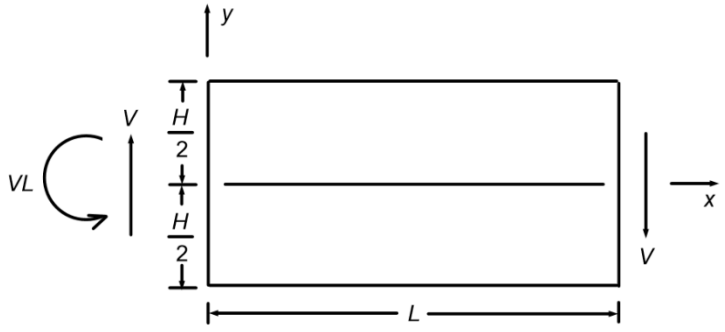

Figure 1. Domain of a cantilever beam.

$$\varepsilon_{xx}=\frac{12VC(1-\nu^*)}{H^3}\,(L-x)y\,,$$
$$\varepsilon_{yy}=-\frac{12VC\nu^*}{H^3}\,(L-x)y\,, \tag{2.3}$$
$$\varepsilon_{xy}=\frac{3VC}{2H^2}\,(4y^2-H^2)\,,$$

where the notation $C=(1+\nu)/E$ has been used. Finally, integrating the strains (2.3), via $\varepsilon_{ij}=(1/2)\big(u_{i,j}+u_{j,i}\big)$, such that $u_x(0,0)=u_y(0,0)=0$ and $u_x(0,H/2)=0$, one obtains the displacement field

$$u_x=\frac{VC}{2H^3}\,[\,12(1-\nu^*)(2Lx-x^2)y+4(2-\nu^*)y^3-(2-\nu^*)H^2y\,]\,,$$
$$u_y=-\frac{VC}{2H^3}\,[\,12\nu^*(L-x)y^2+4(1-\nu^*)(3Lx^2-x^3)+(4+\nu^*)H^2x\,]\,. \tag{2.4}$$

Consistent boundary conditions are then

$$\text{on } x=0\,,\quad \begin{matrix}T_x=-\dfrac{12VL}{H^3}\,y\\ T_y=-\dfrac{3V}{2H^3}\,(4y^2-H^2)\end{matrix}\qquad \text{on } x=L\,,\quad \begin{matrix}T_x=0\\ T_y=\dfrac{3V}{2H^3}\,(4y^2-H^2)\end{matrix}$$
$$\text{and on } y=\pm\frac{H}{2}\,,\quad \begin{matrix}T_x=0\\ T_y=0\end{matrix} \tag{2.5}$$

along with the conditions $u_x(0,0) = u_y(0,0) = 0$ and $u_x(0, H/2) = 0$.

3. Example in Polar Coordinates

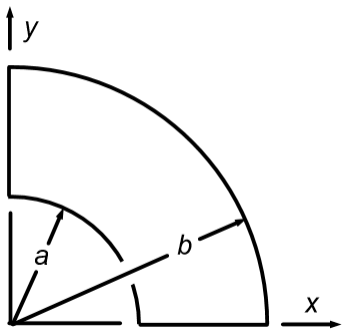

Figure 2. Quarter-annular domain.

In polar coordinates, the quarter-annular domain shown at left in Fig. 2 is subjected to the boundary conditions

$$\begin{aligned} &u_r(a,\theta) = u_\theta(a,\theta) = 0\,, \\ &T_r(b,\theta) = \frac{2F}{b}\cos 4\theta\,, \qquad T_\theta(b,\theta) = 0\,, \\ &T_r(r,0) = 0\,, \qquad u_\theta(r,0) = 0\,, \\ &T_r(r,\pi/2) = 0\,, \qquad u_\theta(r,\pi/2) = 0\,, \end{aligned} \tag{3.1}$$

where

$$F = \int_0^{\pi/8} T_r(b,\theta)\, b\mathrm{d}\theta\,. \tag{3.2}$$

The boundary conditions (3.1) may be satisfied with a displacement field of the form

$$u_r = f(r)\cos 4\theta\,, \qquad u_\theta = g(r)\sin 4\theta\,. \tag{3.3}$$

Substituting eqns. (3.3) into the strain-displacement relations (1.8), one obtains the strains

$$\varepsilon_{rr} = f'\cos 4\theta\,, \qquad \varepsilon_{\theta\theta} = \frac{1}{r}(f + 4g)\cos 4\theta\,, \qquad \varepsilon_{r\theta} = \frac{1}{2}\left(g' - \frac{1}{r}g - \frac{4}{r}f\right)\sin 4\theta\,, \tag{3.4}$$

and via Hooke's Law (1.5) with $C = (1+\nu)/E$, eqns. (3.4) give the stresses

$$\begin{aligned} \sigma_{rr} &= \frac{1}{C(1-2\nu^*)}\left[(1-\nu^*)f' + \frac{\nu^*}{r}f + \frac{4\nu^*}{r}g\right]\cos 4\theta\,, \\ \sigma_{\theta\theta} &= \frac{1}{C(1-2\nu^*)}\left[\nu^* f' + \frac{(1-\nu^*)}{r}f + \frac{4(1-\nu^*)}{r}g\right]\cos 4\theta\,, \\ \sigma_{r\theta} &= \frac{1}{2C}\left(g' - \frac{1}{r}g - \frac{4}{r}f\right)\sin 4\theta\,. \end{aligned} \tag{3.5}$$

Note that eqns. (3.3) and (3.5) satisfy the boundary conditions at $\theta = 0$ and $\theta = \pi/2$ identically. Now, substitution of the stresses (3.5) into the equilibrium eqns. (1.9) yields the coupled pair of ordinary differential equations

$$\begin{aligned} &(1-\nu^*)f'' + \frac{(1-\nu^*)}{r}f' - \frac{(9-17\nu^*)}{r^2}f + \frac{2}{r}g' - \frac{2(3-4\nu^*)}{r^2}g = 0\,, \\ &(1-2\nu^*)g'' + \frac{(1-2\nu^*)}{r}g' - \frac{(33-34\nu^*)}{r^2}g - \frac{4}{r}f' - \frac{4(3-4\nu^*)}{r^2}f = 0\,. \end{aligned} \tag{3.6}$$

By assuming functions of the form

$$f = kr^p\,, \qquad g = lr^p\,, \tag{3.7}$$

eqns. (3.6) become

$$\begin{bmatrix} [\,(1-\nu^*)p^2-(9-17\nu^*)\,] & 2[\,p-(3-4\nu^*)\,] \\ -4[\,p+(3-4\nu^*)\,] & [\,(1-2\nu^*)p-(33-34\nu^*)\,] \end{bmatrix} \begin{bmatrix} k \\ l \end{bmatrix} = \begin{bmatrix} 0 \\ 0 \end{bmatrix}, \tag{3.8}$$

which has nontrivial solutions if the determinant of coefficients is zero, *viz.,*

$$p^4 - 34p^2 + 225 = 0\,. \tag{3.9}$$

Thus,

$$p = -5\,, -3\,, 3\,, 5\,. \tag{3.10}$$

Next, using the four null vectors of eqns. (3.8) as generated by the powers (3.10), one obtains the relations between the eight constants k_i and l_i

$$\begin{aligned} &p=-5 \;\Rightarrow\; l_1 = k_1\,, \qquad p=-3 \;\Rightarrow\; l_2 = \frac{2\nu^*}{3-2\nu^*}k_2\,, \\ &p=3 \;\Rightarrow\; l_3 = -k_3\,, \qquad p=5 \;\Rightarrow\; l_4 = -\frac{2(2-\nu^*)}{1+2\nu^*}k_4\,. \end{aligned} \tag{3.11}$$

Finally, the functions f and g are then

$$f = \frac{k_1}{r^5} + \frac{k_2}{r^3} + k_3 r^3 + k_4 r^5\,, \qquad g = \frac{l_1}{r^5} + \frac{l_2}{r^3} + l_3 r^3 + l_4 r^5\,. \tag{3.12}$$

Turning attention to the boundary conditions at $r = a$ and $r = b$, eqns. (3.3), (3.5), (3.11) and (3.12) give the system

$$\begin{bmatrix} 1/a^5 & 1/a^3 & a^3 & a^5 \\ 1/a^5 & 2\nu^*/[\,(3-2\nu^*)a^3\,] & -a^3 & -2(2-\nu^*)a^5/(1+2\nu^*) \\ -5/b^5 & -9/[\,(3-2\nu^*)b^3\,] & 3b^3 & 5b^5/(1+2\nu^*) \\ -5/b^5 & -6/[\,(3-2\nu^*)b^3\,] & -3b^3 & -10b^5/(1+2\nu^*) \end{bmatrix} \begin{bmatrix} k_1 \\ k_2 \\ k_3 \\ k_4 \end{bmatrix} = \begin{bmatrix} 0 \\ 0 \\ 2FC \\ 0 \end{bmatrix} \tag{3.13}$$

to solve for the constants k_i. The first of eqns. (3.13) is from $u_r(a,\theta) = 0$; the second is from $u_\theta(a,\theta) = 0$; the third, from $T_r(b,\theta) = 2F\cos 4\theta/b$; and the fourth, $T_\theta(b,\theta) = 0$. Instead of solving eqns. (3.13) algebraically, they were solved numerically using the constants

$$E = 3\times 10^7 \text{ psi}\,, \quad \nu = 0.3\,, \quad a = 36 \text{ in}\,, \quad b = 72 \text{ in}\,, \quad F = 10{,}000 \text{ lb} \tag{3.14}$$

for plane stress. The results are

$$\begin{aligned} k_1 &= \;\; 4.468\,854\,986\,101\,9630\times 10^3 & l_1 &= \;\; 4.468\,854\,986\,101\,9630\times 10^3 \\ k_2 &= -6.240\,733\,337\,857\,3010\times 10^0 & l_2 &= -1.134\,678\,788\,701\,3274\times 10^0 \\ k_3 &= \;\; 1.437\,736\,140\,089\,1819\times 10^{-9} & l_3 &= -1.437\,736\,140\,089\,1819\times 10^{-9} \\ k_4 &= -1.194\,905\,134\,758\,0960\times 10^{-13} & l_4 &= \;\; 2.892\,928\,220\,993\,2855\times 10^{-13} \end{aligned}\,, \tag{3.15}$$

which constants solve the problem at hand.

4. The Cell Method

What the author calls "The Cell Method" is not a finite element method, nor is it a finite difference method, but perhaps a hybrid of the two. The author just tried this method because it makes sense, and is simple in its idea. Specifically, it is based on the differentiation cell shown below in Fig. 3. The cell spans the normalized domain $\xi_i \in (-1,1)$. Now, with the aid of the quadratic functions

$$f^0(s) = \frac{1}{2}(-s+s^2)\,, \qquad f^1(s) = 1-s^2\,, \quad f^2(s) = \frac{1}{2}(s+s^2)\,, \tag{4.1}$$

one may construct the nine interpolation functions S^I via

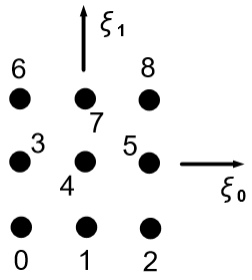

Figure 3. The differentiation cell in normalized $\boldsymbol{\xi}$–space.

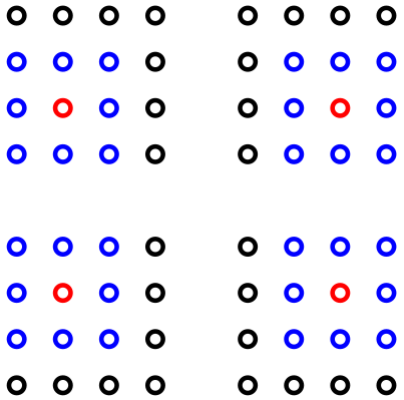

Figure 4. A 4 × 4 computational grid of points containing four differentiation cells.

$$\begin{array}{lll} S^0 = f^0(\xi_0)f^0(\xi_1) & S^1 = f^1(\xi_0)f^0(\xi_1) & S^2 = f^2(\xi_0)f^0(\xi_1) \\ S^3 = f^0(\xi_0)f^1(\xi_1) & S^4 = f^1(\xi_0)f^1(\xi_1) & S^5 = f^2(\xi_0)f^1(\xi_1) \\ S^6 = f^0(\xi_0)f^2(\xi_1) & S^7 = f^1(\xi_0)f^2(\xi_1) & S^8 = f^2(\xi_0)f^2(\xi_1) \end{array} , \tag{4.2}$$

which functions actually are the "shape" functions of the bi-quadratic LaGrange finite element.

The mapping of the differentiation cell to physical **x**–space is achieved via

$$x_i = S^I x_i^I \ , \tag{4.3}$$

where x_i^I are the coordinates of the cell's points. The differentials of eqn. (4.3) are then

$$\mathrm{d}x_i = A_{i\alpha}\mathrm{d}\xi_\alpha \ , \qquad A_{i\alpha} = \frac{\partial x_i}{\partial \xi_\alpha} = S^I_{,\alpha} x_i^I \ , \qquad A_{i\alpha,\beta} = S^I_{,\alpha\beta} x_i^I \ , \tag{4.4}$$

and

$$\mathrm{d}\xi_\alpha = A^{-1}_{\alpha i}\mathrm{d}x_i \ , \qquad A^{-1}_{\alpha i} = \frac{\partial \xi_\alpha}{\partial x_i} \ . \tag{4.5}$$

Now, with the derivative

$$\frac{\partial A^{-1}_{\gamma j}}{\partial \xi_\beta} = -A^{-1}_{\gamma i} A_{i\alpha,\beta} A^{-1}_{\alpha j} \ , \tag{4.6}$$

one finds that the physical gradients of the interpolation functions are, which are obtained via the Chain Rule,

$$S^I_{,j} = S^I_{,\alpha} A^{-1}_{\alpha j} \ , \qquad S^I_{,jk} = \left(S^I_{,\gamma\beta} - S^I_{,\alpha} A_{i\gamma,\beta} A^{-1}_{\alpha i}\right) A^{-1}_{\beta k} A^{-1}_{\gamma j} \ . \tag{4.7}$$

Next, interpolate the displacement vector u_i through the cell with the functions S^I, *viz.,*

$$u_i = S^I u_i^I \ , \qquad u_{i,j} = S^I_{,j} u_i^I \ , \qquad u_{i,jk} = S^I_{,jk} u_i^I \ , \tag{4.8}$$

where u_i^I are the displacements at the cell's points. From Hooke's Law (1.1), $\sigma_{ij} = L_{ijkl} u_{k,l}$, which follows from the symmetries of L_{ijkl}. Into this, substitute the second of eqns. (4.8) to obtain the stresses within the cell

$$\sigma_{ij} = D^I_{ijk} u_k^I \ , \qquad D^I_{ijk} = L_{ijkl} S^I_{,l} \ . \tag{4.9}$$

In particular, also via eqns. (4.8), the equilibrium equation (the second of eqns. 1.7) and the traction vector $T_j = n_i \sigma_{ij}$ are in the cell

$$E^I_{jk}u^I_k = 0\ , \qquad F^I_{jk}u^I_k = T_j\ , \qquad E^I_{jk} = L_{ijkl}S^I_{,li}\ , \qquad F^I_{jk} = n_i L_{ijkl}S^I_{,l}\ . \tag{4.10}$$

Turning attention to Fig. 4 above, the computational procedure of the cell method is as follows. Figure 4 shows four copies of the same 4×4 computational grid of points. In each copy, in blue and red, are shown the four differentiation cells. Note that the cells overlap. First, at each of the four internal (red) points of the grid, two algebraic equations are constructed by evaluating the equilibrium equations at point 4 of each cell (via the operator in the first of eqns. 4.10). Two algebraic equations for each of the remaining 12 points are then supplied by the boundary conditions, by either prescribing u_i or the traction vector T_j (via the operator in the second of eqns. 4.10). Note that the boundary conditions are applied at either the points 1, 3, 5 or 7 of the cell (unless the boundary point is on a corner, for which the boundary conditions are applied at either the points 0, 2, 6 or 8 of the cell). In any case, a 32×32 system of equations has been constructed, which system may be solved for the 32 nodal displacements.

5. Numerical Example in Rectangular Coordinates

Here the problem solved analytically in Sec. 2 is solved numerically. The values of the constants used in the analysis are

$$L = 10\ \text{in}\ , \qquad H = 5\ \text{in}\ , \qquad E = 3.0 \times 10^7\ \text{psi}\ , \qquad \nu = 0.3\ , \qquad V = 10\,000\ \text{lb/in} \tag{5.1}$$

and plane stress is assumed. The computational grid used in the analysis is shown below in Fig. 5. It consists of a 37×25 array of 925 points, and a 35×23 array of 805 overlapping differentiation cells.

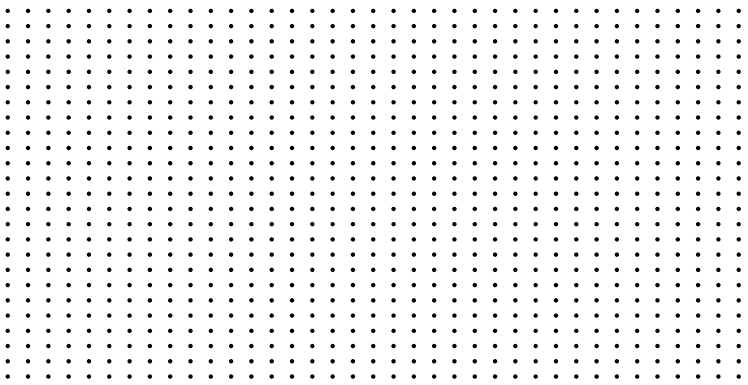

Figure 5. Computational grid used in the analysis.

In the graphs in Figs. 6 through 11 below, the solid curves represent the exact solution; and the plotted points, the calculated numerical solution.

The displacement components along the bottom surface of the beam at $y = -H/2$ are shown in Fig. 6 below. As is seen, the numerical solution is quite accurate.

Figure 7 below shows the displacement components along the left face of the beam at $x = 0$. Here, the numerically calculated values of u_x are somewhat inaccurate. Nevertheless, the magnitudes of the displacements in Fig. 7 are 100 times smaller than the those in Fig. 6. Thus, the absolute error in the calculated values is not that bad. On the other hand, the numerically calculated values of u_y are quite accurate (except for a minor error at $y = H/2$).

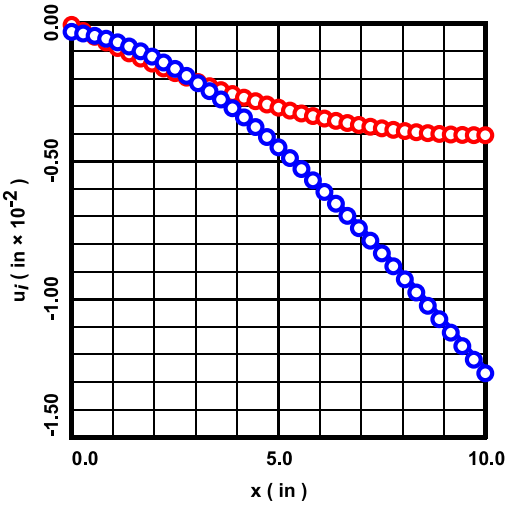

Figure 6. Displacement components u_x (red) and u_y (blue) at $y = -H/2$.

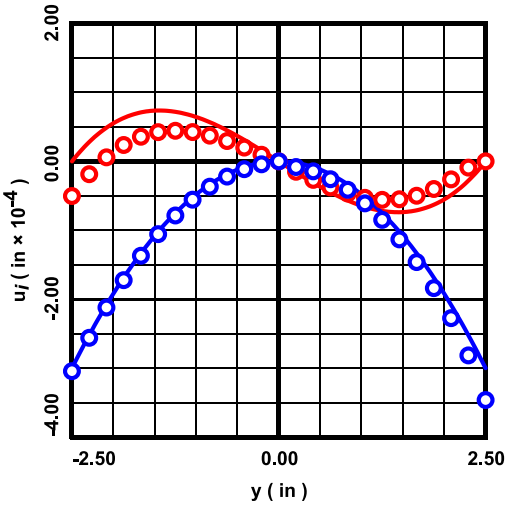

Figure 7. Displacement components u_x (red) and u_y (blue) at $x = 0$.

Figure 8 below shows the displacement components along the right face of the beam at $x = L$. As is evident, these numerical results are quite accurate.

The stress components along the left face of the beam at $x = 0$ are shown below in Fig. 9. As before, except for the slight error in σ_{xx} at $y = H/2$, the numerical results are quite accurate.

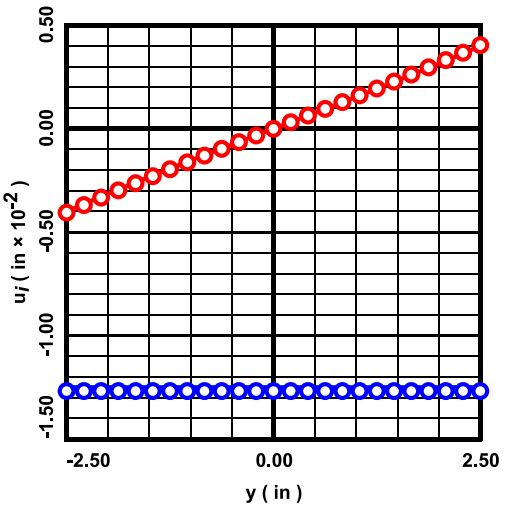

Figure 8. Displacement components u_x (red) and u_y (blue) at $x = L$.

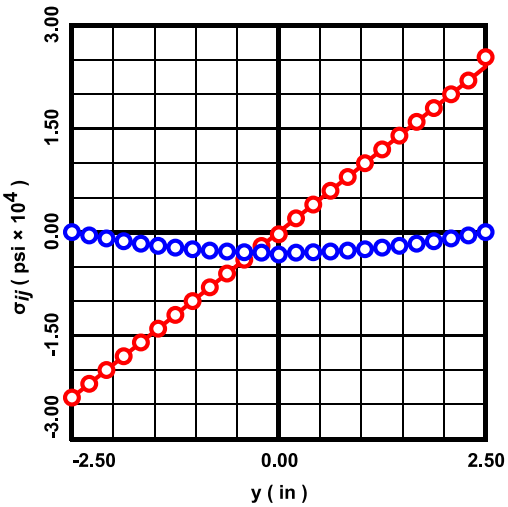

Figure 9. Stress components σ_{xx} (red) and σ_{xy} (blue) at $x = 0$.

Figure 10 below shows the numerically calculated stress component σ_{xy} along the right face of the beam at $x = L$, which numerical results are very accurate.

Finally, the stress components σ_{xx} and σ_{xy} along the vertical line of grid points located at $x = 3L/4$ is shown at below right in Fig. 11. As was the case with Fig. 10, here also the numerical results are highly accurate.

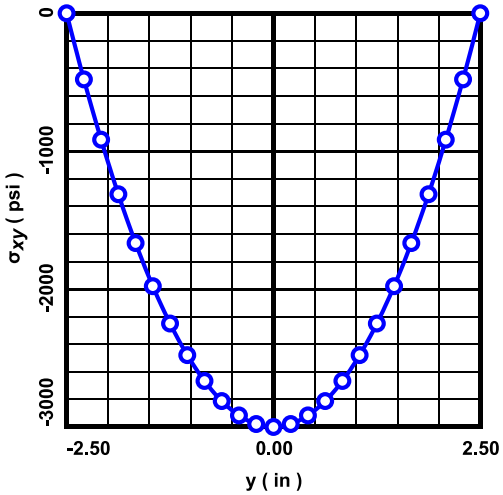

Figure 10. Stress component σ_{xy} at $x = L$.

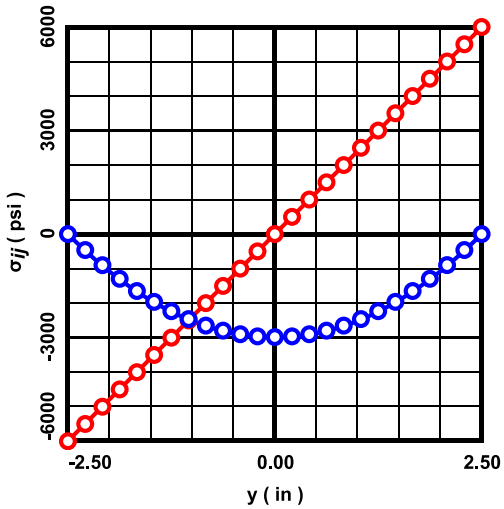

Figure 11. Stress components σ_{xx} (red) and σ_{xy} (blue) at $x = 3L/4$.

Overall, for this problem, the performance of the cell method is quite acceptable.

6. Numerical Example in Polar Coordinates

The problem solved analytically in Sec. 3 above is analyzed here numerically. The constants used in the analysis were given previously in eqn. (3.14). The computational grid used in the analysis is shown below in Fig. 12. It consists of a 25 (radial) × 37 (circumferential) array of 925 points, and a 23 (radial) × 35 (circumferential) array of 805 overlapping differentiation cells.

Figure 13 below shows the numerical results for the displacement component u_x along the bottom boundary of the domain at $\theta = 0$. As the figure shows, the calculations are quite accurate.

The displacement components along the outer circumference of the domain at $r = b$ are shown below in Fig. 14. Once again, the numerical results are highly accurate.

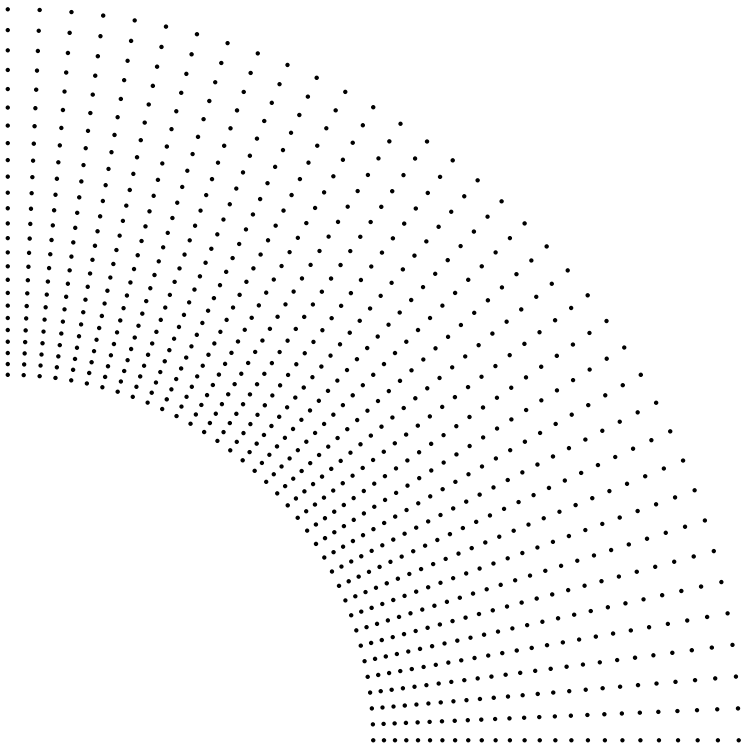

Figure 12. Computational grid used in the analysis.

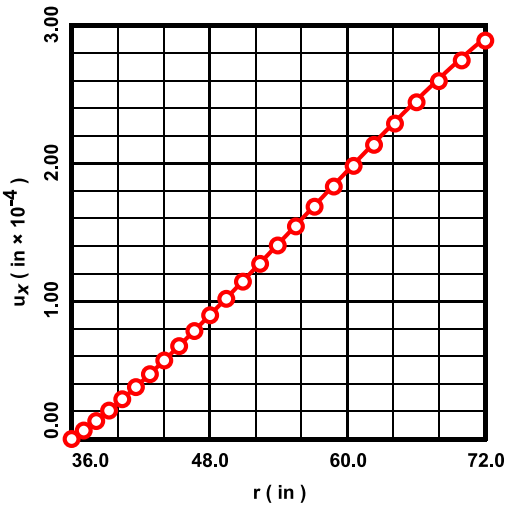

Figure 13. Displacement component u_x at $\theta = 0$.

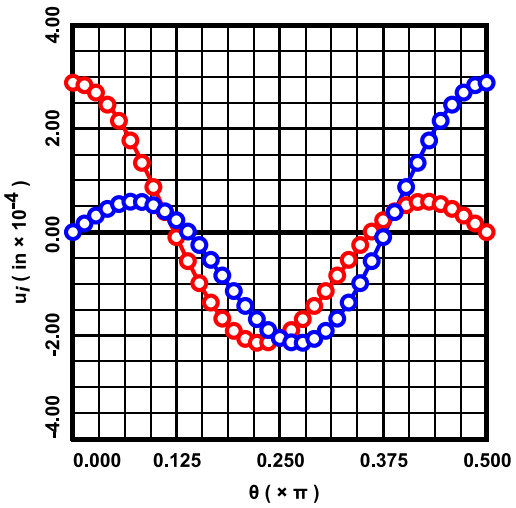

Figure 14. Displacement components u_x (red) and u_y (blue) at $r = b$.

The numerically calculated displacement components along the radial line of grid points located at $\theta = \pi/8$ is shown below in Fig. 15. As is seen, the numerical results are acceptably accurate.

Figure 16 below shows the results of the calculation for the stress components σ_{xx} and σ_{yy} along the bottom surface of the domain at $\theta = 0$. Here the numerical results basically correspond to the exact analytical solution.

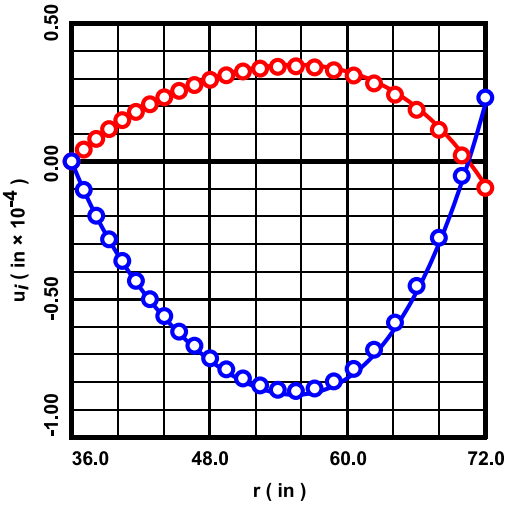

Figure 15. Displacement components u_x (red) and u_y (blue) at $\theta = \pi/8$.

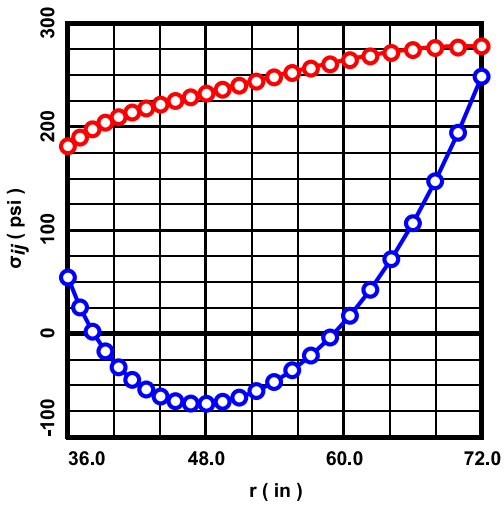

Figure 16. Stress components σ_{xx} (red) and σ_{yy} (blue) at $\theta = 0$.

The stress components along the outer circumference of the domain at $r = b$ are given at below left in Fig. 17. As was the case for Fig. 16, here the numerical calculations basically reproduce the exact solution.

Finally, Fig. 18 at below right shows the numerically calculated stress components along the radial line of grid point located at $\theta = \pi/8$. Here, the numerical results are quite accurate. One notes that, at $\theta = \pi/8$, $\sigma_{xy} = \sigma_{yy}$.

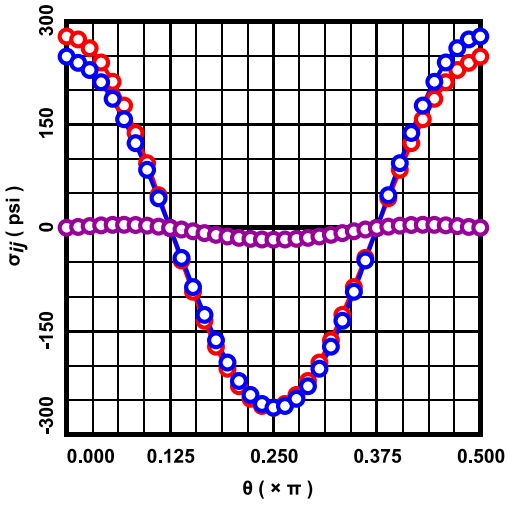

Figure 17. Stress components σ_{xx} (red), σ_{yy} (blue) and σ_{xy} (purple) at $r = b$.

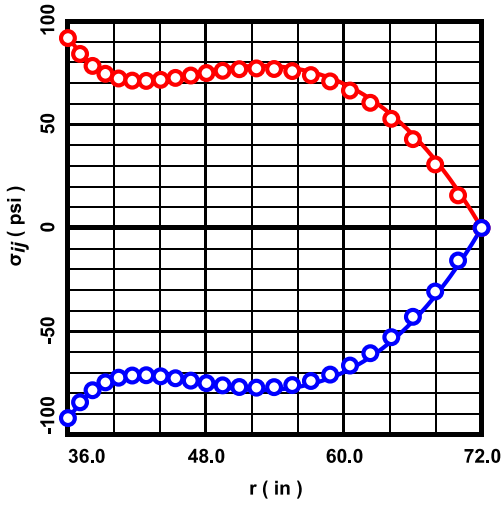

Figure 18. Stress components σ_{xx} (red) and σ_{yy} (blue) at $\theta = \pi/8$.

Overall, for this problem, the performance of the cell method is highly reliable.

7. Closing Remarks

While the author has not seen this method before, as mentioned above in Sec. 4, he tried it out just because it makes sense, and because the idea behind it is quite simple. It is perhaps easier to implement than the finite element method, because no integrations are required. In any case, the above considerations show that, for two-dimensional linear elasticity, the cell method is quite effective and reliable.